Periodic Orbits of Spatial Kepler Problem

Dongho Lee

April 25, 2025

SNU, RIM

Background and Collaborators

- Developed result of "The Conley-Zehnder indices of the rotating Kepler problem" by Albers, Fish, Frauenfelder, van Koert, 2013, which deals with planar rotating Kepler problem.
- Based on my ph.D thesis.
- Collaborator: Beomjun Sohn

Contents

Rotating Kepler Problem

Kepler Problem

The **Kepler problem** describes the motion of an object under the gravitational force of a mass at the origin.

Hamiltonian : **Kepler energy** $E : T^*(\mathbb{R}^3 \setminus \{0\}) \to \mathbb{R}$,

$$E(q,p) = \frac{1}{2}|p|^2 - \frac{1}{|q|}$$

The singularity at 0 will be regularized by Moser regularization.

Planar problem : domain is $T^*\mathbb{R}^2 \setminus \{0\}$.

Three Laws of Kepler

In 17C, Kepler discovered these three laws through observation.

1. The solutions are conic sections with one focus at the origin.
   If $E < 0$, every orbit is an ellipse.
2. The areal velocity $d\text{Area}/dt = r^2\dot{\theta}/2$ is constant.
3. The period τ of solution satisfies $\tau^2 = -\pi^2/2E^3$.
   τ only depends on the Kepler energy.

Two Invariants

1. **Angular momentum** $L = q \times p$.
   - Direction of $L =$ Normal to the plane which the orbit contained in.
2. **Laplace-Runge-Lenz vector** $A = p \times L - \frac{q}{|q|}$
   - Direction of $A =$ Direction of the major axis
   - Length of $A =$ Eccentricity ε

Some relations :

1. $\{E, L_i\} = \{E, A_j\} = 0$ for any i, j.
2. $\{|L|, L_i\} = 0$ for any i.
3. $\{L_i, A_j\} = \varepsilon_{ijk} A_k$. In particular, $\{L_i, A_i\} = 0$
4. $\varepsilon^2 = |A|^2 = 2E|L|^2 + 1$.

Two Invariants

On $L \cdot q$, the Kepler orbit is given in the polar coordinate by

$$r = \frac{|L|^2}{1 + |A|\cos(\theta - g)} \quad (g \text{ is determined by the direction of } A).$$

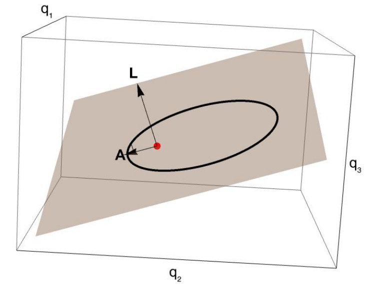

In particular, E, L and A determine the Kepler orbit.

Moser Regularization

For $E_0 < 0$, we can embed the Hamiltonian flow on the level set $E^{-1}(E_0)$ into the unit geodesic flow on T^*S^3.

$\Rightarrow$ Compactification of the energy level set by $ST^*S^3 \simeq S^3 \times S^2$.

The **collision orbits** are added.

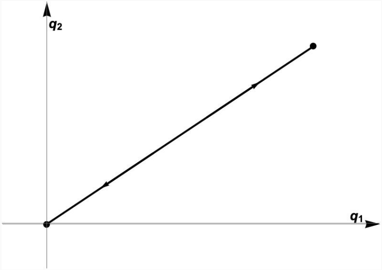

This is a special case of ellipse with $\varepsilon = |A| = 1$, $L = 0$.

Rotating Kepler Problem

Kepler problem : Every orbit is periodic $\Rightarrow$ Too degenerate.

(Real motivation: a limit of the restricted three-body problem)

Rotating Kepler problem is defined by Hamiltonian

$$H = E + L_3 = \frac{1}{2}|p|^2 - \frac{1}{|q|} + (q_1 p_2 - q_2 p_1).$$

H : **total energy** or **Jacobi energy** (usually, $H = c$)

E : **Kepler energy**.

Note. Moser regularization is still valid, gives a Finsler geodesic flow on T^*S^3, and the energy hypersurface is $ST^*S^3 \simeq S^3 \times S^2$.

Periodic Orbits of Rotating Kepler Problem

Periodic Orbits

There are three types of periodic orbits.

1. Two planar circular orbits, nondegenerate for generic c.
2. Two vertical collision orbits, nondegenerate for generic c.
3. Morse-Bott family of degenerate orbits with specific Kepler energy.

Idea. Fl^{L_3} is a rotation along q_3- and p_3-axis, and $Fl^H = Fl^E \circ Fl^{L_3}$.

Nondegenerate Periodic Orbits

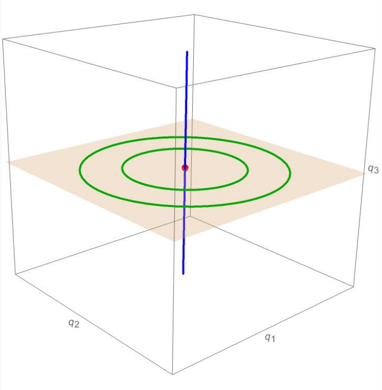

Figure 1: Planar circular orbits and vertical collision orbits

These are periodic after composing with Fl^{L_3}.

Nondegenerate Periodic Orbits

Circular condition: $\varepsilon^2 = 2EL_3^2 + 1 = 2E(c-E)^2 + 1 = 0.$

For fixed $c < -3/2$, there are 3 **planar circular orbits** with different E.

1. **Retrograde orbit** γ_+: $L_3 > 0$, smaller E and smaller radius.
2. **Direct orbit** γ_-: $L_3 < 0$, larger E and larger radius.
3. The rest one, outer direct orbit, lies on the unbounded component, and not of our interest (discarded during regularization).

Vertical collision orbits $\gamma_{c_\pm}$: $L = 0$, $A_3 = \mp 1$, $c = E$.

- They do not appear in the planar problem.

At generic c, these orbits and their covers are isolated, so nondegenerate.

Diagram of the Nondegenerate Orbits

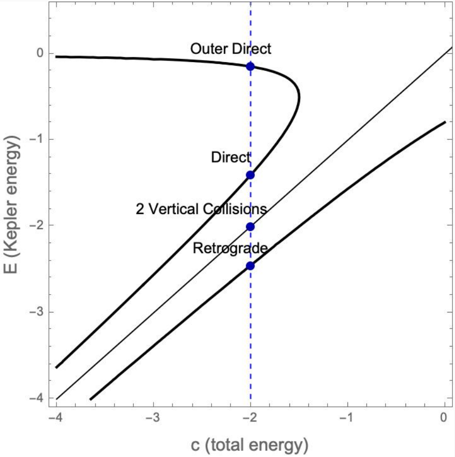

Figure 2: Graph of $2E(c-E)^2+1=0$ and the orbits

Morse-Bott Family

For other cases, the periods of E-orbit and L_3-orbit must be the same.

$\tau = 2\pi/(-2E)^{3/2} \Rightarrow$ there exists some $k, l \in \mathbb{Z}$ such that

$$k\tau = \frac{2k\pi}{(-2E)^{3/2}} = 2l\pi \;\Rightarrow\; E_{k,l} = -\frac{1}{2}\left(\frac{k}{l}\right)^{2/3}$$

For given c, only orbits with Kepler energy $E_{k,l}$ can be periodic.

Such orbits appear with Morse-Bott S^3-family $\Sigma_{k,l}$. (will be explained)

Note. We have S^1-families in the planar problem.

Morse-Bott Family

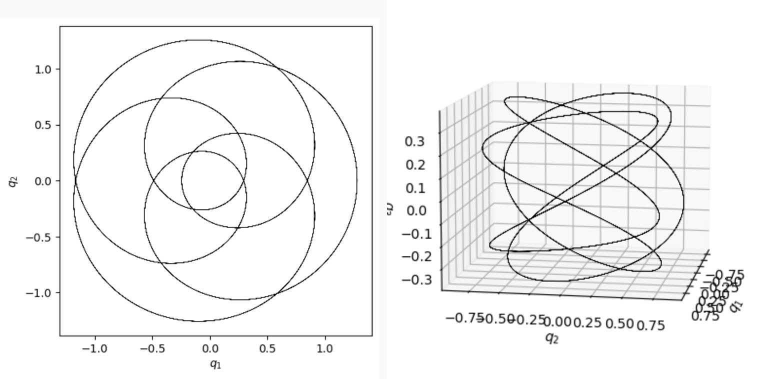

Figure 3: Illustration of periodic orbits on a plane and space [1]

[1] Chankyu Joung drew these nice pictures.

Moduli Space

Recall. E, L and A characterizes the Kepler orbit.

Denote $x = \sqrt{-2E}L - A$, $y = \sqrt{-2E}L + A$.
$\Rightarrow |x|^2 = |y|^2 = -2E|L|^2 + |A|^2 = 1$.

The moduli space of the Kepler orbits with Kepler energy E is

$$\mathcal{M}_E = \left\{(x, y) \,:\, |x|^2 = |y|^2 = 1\right\} \simeq S^2 \times S^2.$$

(Space of unit geodesics of S^3) $= ST^*S^3/S^1 \simeq S^2 \times S^2$.

Note. In the planar problem, the moduli space is $\mathbb{RP}^3/S^1 \simeq S^2$.

Properties of $\mathcal{M}_E$

$L_3 = (x+y)/\sqrt{-2E}$ serves as a Morse function with 4 critical points.

1. The direct orbit $\gamma_- = (-1,-1)$ has index 0.
2. Vertical collision orbits $\gamma_{c_\pm} = (\pm 1, \mp 1)$ have index 2.
3. The retrograde orbit $\gamma_+ = (1,1)$ has index 4.

Every regular level set of L_3 is S^3.

$\Rightarrow$ Morse-Bott family in the rotating Kepler problem.

(For fixed c, if $E = E_{k,l}$, then $L_3 = c - E_{k,l}$ is specified.)

Properties of $\mathcal{M}_E$

A_3 also serves as a Morse function.

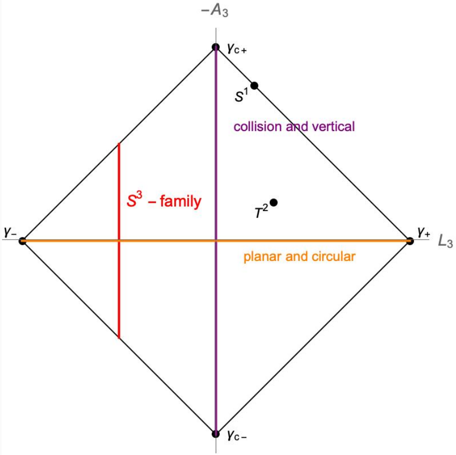

Figure 4: Toric-style diagram of $\mathcal{M}_E$.

Periodic Orbits in $H^{-1}(c)$

For generic energy level c, the energy hypersurface $H^{-1}(c)$ contains 4 nondegenerate orbits and (infinitely many) Morse-Bott S^3-families.

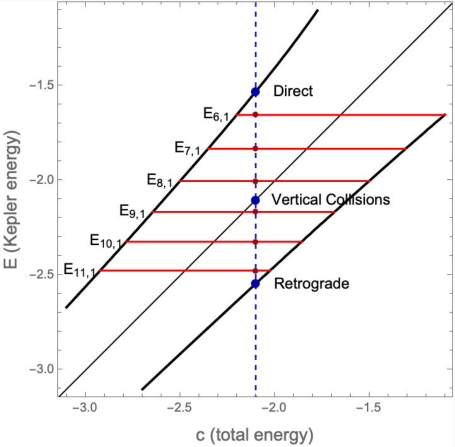

Conley-Zehnder Indices of Kepler Orbits

Conley-Zehnder Index of Planar Circular Orbits

Theorem

Let $\gamma_\pm$ be the retrograde and direct orbits of Kepler energy E where $E \neq E_{k,l}$ for any k, l. Then $\gamma_\pm$ and their multiple covers are non-degenerate. The Conley-Zehnder index of N-th iterate of $\gamma_\pm$ is

$$\mu_{CZ}(\gamma_\pm^N) = 2 + 4 \max \left\{ n \in \mathbb{Z}_{>0} : n < N \frac{(-2E)^{3/2}}{(-2E)^{3/2} \pm 1} \right\}$$
$$= 2 + 4 \left\lfloor N \frac{(-2E)^{3/2}}{(-2E)^{3/2} \pm 1} \right\rfloor$$

The index is exactly the twice compare to the planar problem, which was computed in [AFFvK13].

Conley-Zehnder Index of Planar Circular Orbits

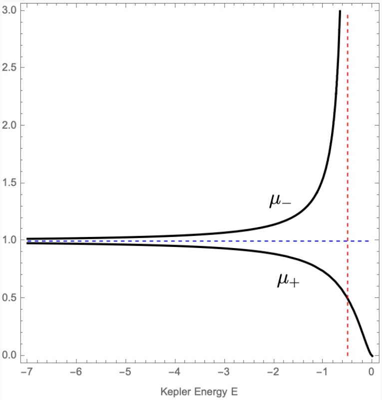

Figure 5: Graph of $\mu_\pm = \frac{(-2E)^{3/2}}{(-2E)^{3/2} \pm 1}$.

The index of γ_+^N decreases by 4, while γ_-^N increases by 4, whenever $\mu_\pm$ touches $k/N \Leftrightarrow E = E_{N-k,k}$ or $E = E_{N+k,k}$. (bifurcation!)

Conley-Zehnder Index of Vertical Collision Orbits

Theorem

Let $\gamma_{c_\pm}$ be the vertical collision orbits of Kepler energy E where $E \neq E_{k,l}$ for any k, l. Then $\gamma_{c_\pm}$ and their multiple covers are non-degenerate. The Conley-Zehnder index of N-th iteration of $\gamma_{c_\pm}$ is

$$\mu_{CZ}(\gamma_{c_\pm}^N) = 4N.$$

In particular, change of the energy does not change the index.

Summary of the Result

Orbits	Initial Index	Index Change
Retrograde γ_+^N	$4N-2$ if $E < E_{N-1,1}$	-4 at $E = E_{N-k,k}$ for $k = 1, \ldots, N-1$ $= 2$ if $E > E_{1,N-1}$.
Direct γ_-^N	$4N+2$ if $E < E_{N+1,1}$	$+4$ at $E = E_{N+k,k}$ for $k = 1, 2, \ldots$
Vertical Collisions $\gamma_{c_\pm}^N$	$4N$	No change

Table 1: Conley-Zehnder indices of nondegenerate orbits

First bifurcation of $\gamma_\pm^N$ is at $c = E_{N\mp1,1} \pm 1/\sqrt{-2E_{N\mp1,1}}$.

Interpretation by Symplectic Homology

$$SH_*^{+,S^1}(T^*S^3) \simeq \begin{cases} \mathbb{Z}_2 & * = 2, \\ \mathbb{Z}_2^2 & * = 2k \geq 4, \\ 0 & \text{otherwise.} \end{cases}$$

For fixed N, there exists $c \ll -3/2$ such that $H^{-1}(c)$ consists of

1. $k(\leq N)$-th covers of $\gamma_\pm$ of index $4k \mp 2$. (No bifucation)
2. Higher covers have index $> 4N + 2$.

Up to degree $4N + 2$, we have

1. One generator at degree 2. (γ_+.)
2. Two generators at degree 6, 10, 14, $\cdots$, $4N + 2$. (γ_+^{k+1} and γ_-^k.)
3. Two generators at degree 4, 8, 12, $\cdots$, $4N$. ($\gamma_{c_+}^k$ and $\gamma_{c_-}^k$.)

This describes $SH_*^{+,S^1}(T^*S^3)$ up to degree $4N + 2$ completely.

Morse-Bott Spectral Sequence

Case : Reeb orbits with the same period τ form a submanifold Σ which satisfies **Morse-Bott condition** : $\det(dFl_\tau^{X_H}|_{\nu\Sigma} - \mathrm{Id}|_{\nu\Sigma}) \neq 0.$

Theorem

There exists a spectral sequence converging to $SH^{+,S^1}(W)$ *whose* E^1*-page is given by*

$$E^1_{pq}(SH^{S^1,+}) = \begin{cases} \bigoplus_{\Sigma \in C(p)} H^{S^1}_{p+q-\mathrm{shift}(\Sigma)}(\Sigma) & p > 0 \\ 0 & p \leq 0 \end{cases}$$

where $\mathrm{shift}(\Sigma) = \mu_{RS}(\Sigma) - \frac{1}{2}\dim \Sigma / S^1$.

Morse-Bott Property

We compute the linearized return map by using action-angle coordinates.

In the planar problem, [AFFvK13] used **Delaunay coordinate** given by $(p_l, p_g) = (1/\sqrt{-2E}, L_3)$, which degenerate at planar circular orbits.

In the spatial problem, we should use two coordinates:

1. Delaunay coordinate : $(p_l, p_g, p_\theta) = (1/\sqrt{-2E}, |L|, L_3)$.

   But this coordinate system degenerates at every planar orbit.
2. **LRL coordinate** : $(p_l, p_\eta, p_\theta) = (1/\sqrt{-2E}, A_3, L_3)$.

   This degenerates at every circular orbit, but covers planar orbits.

Conley-Zehnder Index of Degenerate Orbits

As we increase the Kepler energy level E from $E_{k,l} - \varepsilon$ to $E_{k,l} + \varepsilon$,

1. Retrograde: $\mu_{CZ}(\gamma_+^{k+l})$ decreases from $4k+2$ to $4k-2$.
2. Direct: $\mu_{CZ}(\gamma_-^{k-l})$ increases from $4k-2$ to $4k+2$.
3. Morse-Bott family: At $E = E_{k,l}$, S^3-family $\Sigma_{k,l}$ emerges.

Theorem

Index of S^3-family $\Sigma_{k,l}$ with Kepler energy $E_{k,l}$ is

$$\begin{aligned}\mu_{CZ}(\Sigma_{k,l}) &= \mathrm{shift}(\Sigma) + \dim S^3/2 \\ &= (4k-2) + 3/2 = 4k - 1/2.\end{aligned}$$

Conley-Zehnder Index of Degenerate Orbits

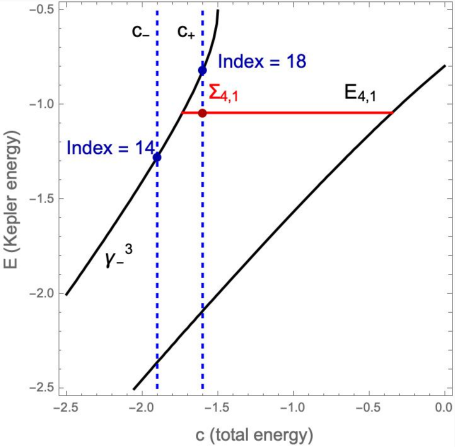

Figure 6: Bifurcation diagram of γ_-^3 at $E = E_{4,1}$

Morse-Bott Spectral Sequence

(Local) Morse-Bott spectral sequence of $SH^{S^1,+}$

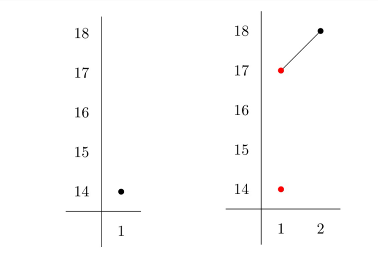

Left: $H = c_-$, triple cover of direct orbit with index 14.

Right: $H = c_+$, triple cover of direct orbit with index 18,

$\Rightarrow S^3$-family must have shift 14, so $\mu_{CZ}(\Sigma_{4,1}) = 14 + 3/2 = 15.5$.

Questions / Comments / Suggestions

Appendix 1. Hill's Region

$$H(q,p) = \underbrace{\frac{1}{2}\left((p_1 - q_2)^2 + (p_2 + q_1)^2\right)}_{\text{nonnegative}} + \underbrace{\left(-\frac{1}{|q|} - \frac{q_1^2 + q_2^2}{2}\right)}_{\text{effective potential } U(q)}$$

$H = c \Rightarrow U(q) \leq c$, and $\{q : U(q) \leq c\}$ is called a **Hill's region**.

If $c < -3/2$, the Hill's region has a bounded component (red ball).

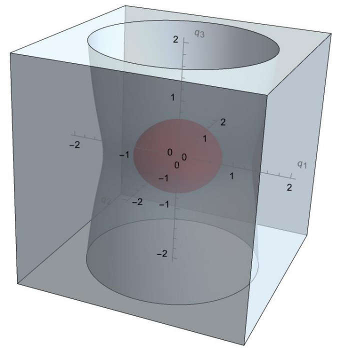

Appendix 2. Moser Regularization

Fix $E = E_0$. Consider the Hamiltonian on $T^*\mathbb{R}^3$

$$\tilde{K}(q,p) = \frac{1}{2}\left(|q|\left(E(q,p) - E_0\right) + 1\right)^2 = \frac{1}{2}\left(\frac{1}{2}(|p|^2 - 2E_0)|q|\right)^2.$$

This is the Hamiltonian of geodesic vector field on $T^*S^3_r$ under the stereographic projection

$$\begin{aligned} \Phi_r : T^*S^3_r &\to T^*\mathbb{R}^3 \\ (x,y) &\mapsto \left(\frac{r\vec{x}}{r - x_0}, \frac{r - x_0}{r}\vec{y} + \frac{y_0}{r}\vec{x}\right) \end{aligned}$$

where $r = \sqrt{-2E_0}$, composed with a switch map $(q,p) \mapsto (-p,q)$.

Appendix 2. Moser Regularization

On $T_r^*S^3$, we have

$$K_r = \frac{r^4}{2}|y|^2$$

The level set $E^{-1}(E_0)$ can be embedded into $K^{-1}(1/2)$

$\Rightarrow$ Kepler Hamiltonian vector field and geodesic vector field are parallel.

$$X_K|_{E^{-1}(E_0)}(p,q) = |q|X_E|_{E^{-1}(E_0)}(-q,p).$$

We regard Kepler problem as a sub-system of the geodesic flow on T^*S^3.

Appendix 3. Restricted Circular Three-body Problem

Restricted circular three-body problem describes a motion of a massless body under the gravitational force of two objects with mass ratio μ, and assume the motions of two bodies are circular.

Corresponding Hamiltonian is time-dependent.

$$E_t(q,p) = \frac{1}{2}|p|^2 - \frac{\mu}{|q-m(t)|} - \frac{1-\mu}{|q-e(t)|},$$
$$e(t) = -\mu(\cos t, -\sin t, 0),\ m(t) = (1-\mu)(\cos t, -\sin t, 0)$$

In rotating frame, the Hamiltonian is autonomous (time-independent).

$$H = \frac{1}{2}|p|^2 - \frac{\mu}{|q-(1-\mu)|} - \frac{1-\mu}{|q-\mu|} + (q_1p_2 - q_2p_1)$$

Rotating Kepler problem is a limit case, $\mu = 0$.

Appendix 3. Restricted Circular Three-body Problem

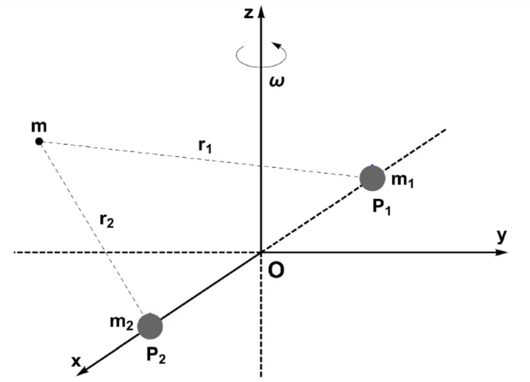

Figure 7: Restricted circular three-body problem[2]

[2] H. Alrebdi, F.Dubeibe, K,Papadakis, E.Zotos "Equilibrium dynamics of a circular restricted three-body problem with Kerr-like primaries"

Appendix 4. How to compute the CZ index?

1. For nondegenerate orbits, find a parametrization and period.
2. Find symplectic frame which can be extended to the capping disk.
   - For planar circular orbits, an appropriate global frame in $T^*\mathbb{R}^2$ was introduced in [AFFvK13]. We extended the frame to $T^*\mathbb{R}^3$.
   - For vertical collision orbits, we used other frame.
3. Compute the linearized flow and crossing forms.
   - For vertical collision orbits, we splitted the flow into E-part and L_3-part. For the singularity of E-part, we used a limit argument.
4. Use Morse-Bott spectral sequence to compute the index of degenerate orbits.

Appendix 5. Result in the Planar Problem

Theorem (AFFvK13)

Let $\gamma_\pm$ be the retrograde and direct orbits of Kepler energy E where $E \neq E_{k,l}$ for any k, l. Then $\gamma_\pm$ and their multiple covers are non-degenerate. The Conley-Zehnder index of N-th iterate of $\gamma_\pm$ is

$$\begin{aligned}\mu_{CZ}(\gamma_\pm^N) &= 1 + 2\max\left\{n \in \mathbb{Z}_{>0} : n < N\frac{(-2E)^{3/2}}{(-2E)^{3/2} \pm 1}\right\} \\ &= 1 + 2\left\lfloor N\frac{(-2E)^{3/2}}{(-2E)^{3/2} \pm 1}\right\rfloor\end{aligned}$$

This shows the dynamical convexity of the planar rotating Kepler problem. (The energy hypersurface is $\mathbb{RP}^3$, and the retrograde orbit is non-contractible but its double cover is.)

Thank you for your attention!